Sine wave measurements of SPRITE detector MTF

Kenneth J. Barnard and Glenn D. Boreman

University of Central Florida
Electrical Engineering Department
Center for Research in Electro-Optics and Lasers
Orlando, Florida 32816

Allen E. Plogstedt and Barry K. Anderson

McDonnell Douglas Missile Systems Company
701 Columbia Boulevard
Titusville, Florida 32780

ABSTRACT

A method is presented for measuring the modulation transfer function of SPRITE detectors with a HgCdTe composition optimized for the 3-5 μm band. This method incorporates a 3.39 μm HeNe laser to generate Young's fringes of varying spatial frequency, which are scanned across the detector elements. The results are consistent with theoretical models for these devices and indicate a limited resolution capability for SPRITEs used for the 3-5 μm band.

1. INTRODUCTION

The SPRITE (signal processing in the element) detector is a device used in serial scan thermal imaging systems that performs an internal time-delay-and-integration (TDI) operation on photogenerated carriers to improve signal-to-noise ratio (SNR) without complex external electronics.[1,2] The three-terminal n-type HgCdTe device is shown in Fig. 1. An applied electric field across the structure from a constant current source causes photogenerated carriers to drift along the bar with an ambipolar velocity v_a. The infrared image is mechanically scanned at a velocity v_s that matches the ambipolar drift velocity. As the image is scanned, the signal adds coherently and the noise adds incoherently to produce an enhancement of the SNR at the readout terminal. This TDI is performed without external circuitry to implement delay-line and summation operations, thus reducing system complexity.

Resolution of SPRITE detectors is limited by both carrier diffusion and readout geometry.[3] We will present a method of measuring the modulation transfer function (MTF) of SPRITEs fabricated for operation over the 3-5 μm band. A 3.39 μm HeNe laser is used to generate Young's fringes of varying spatial frequency that are mechanically scanned across the SPRITEs. MTF is determined from the modulation depth of the output signal. Various length SPRITE detectors with tapered and bifurcated readout geometries are studied. The measured MTFs are compared to the theoretical predictions[4,5] of MTF based on detector geometry and operating parameters.

2. EQUIPMENT

The setup used for the MTF measurements is shown in Fig. 2. The laser source was a 3.39 μm HeNe laser with a linearly polarized TEM_{00} output power of 25 mW. Output power was adjusted using a wire grid polarizer. After expansion to a 25 mm diameter, the beam was focused on a dual-pinhole aperture to produce Young's fringes. Different apertures provided various spatial frequency fringes. A 10-sided rotating polygon mirror performed the scanning operation of the fringes across the SPRITE bars. The output of the detector was amplified using a low noise pre-amp and the modulation depth of the signal was measured on an oscilloscope.

The pinhole apertures were designed based on flux throughput, the required spatial frequency of the fringes at the detector plane, and the acceptable diffraction envelope due to the diameter of the holes. Based on a 20 cm

 0-8194-0597-3/91/$4.00

aperture-to-detector distance, the spacing of the pinholes was chosen to be 1.0 to 4.0 mm in steps of 0.5 mm. These choices produced spatial frequencies up to ~6 cyc/mm. The diameter of the pinholes was chosen to give the largest diffraction envelope at the detector plane while still allowing a reasonable flux throughput. Based on these considerations, a pinhole diameter of 100 μm was used for these measurements.

The SPRITE detectors were packaged in an enclosure with a Sapphire window. This package was housed in a LN_2 dewar with a $CaCl_2$ window. For all of the MTF measurements, the detectors were held at a temperature of 190°K.

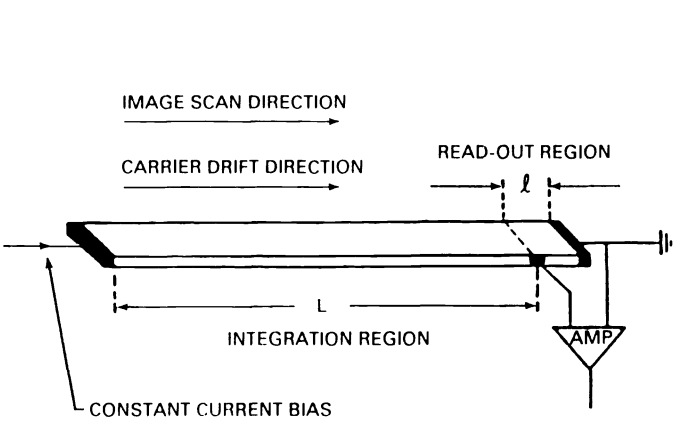

Fig. 1. SPRITE detector geometry.

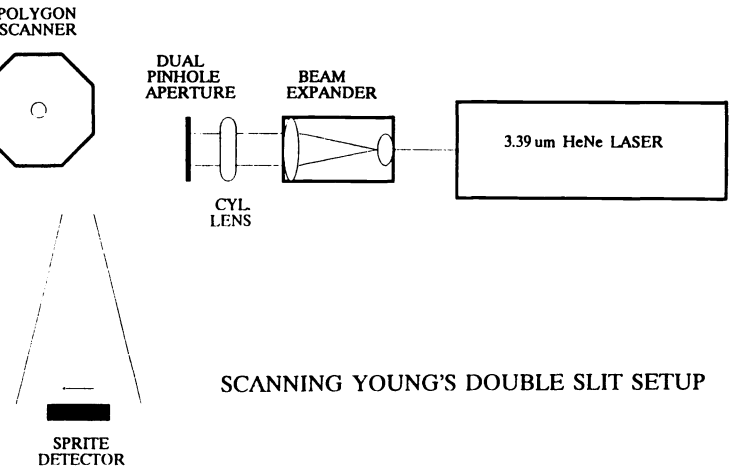

Fig. 2. Measurement setup.

3. SYSTEM CALIBRATION

A calibration procedure was necessary prior to each particular spatial frequency measurement in order to maintain a constant modulation depth of the fringes incident on the detectors. For each spatial frequency measurement, the polygon scanner was removed and a Ge lens was used to image the illuminated pinhole aperture onto a pyroelectric vidicon. The laser output was chopped at 8 Hz for proper vidicon imaging. The video output of the vidicon was examined on a line-by-line basis in the vicinity of the pinhole signal and the pinhole aperture was positioned to produce maximum and equal signal levels for both pinholes. By maintaining an equal flux output from both pinholes, a constant input modulation could be guaranteed for all measurements. After completing the calibration, the polygon scanner was replaced and positioned to give the best output signal from the SPRITEs.

4. MTF MEASUREMENTS

SPRITE detector bias conditions for the MTF measurements were based on a fixed scan velocity of 67 m/s for the optical signal across the detectors. The value of the bias field across the detector needed to produce the required scan velocity is found from the ambipolar drift velocity of the carriers in the material and is given by the relation

$$v_a = \mu_a E , \qquad (1)$$

where μ_a is the ambipolar mobility and E is the electric field across the bar. Using a previously published value for mobility in 3-5 μm optimized HgCdTe (Ref. 2) of $\mu_a \approx 150$ $cm^2/v{\cdot}sec$ gives E = 44.7 v/cm. This value of the bias electric field was used for all measurements. Initially, the polygon scanner velocity was set to give the correct scan velocity based on the distance between the scanner and detector plane. The scanner velocity was then fine tuned until the maximum output modulation from the SPRITEs was obtained. A typical detector output for an input spatial frequency of 4.3 cyc/mm is shown in Fig. 3. The modulation depth was measured at the point where the diffraction envelope peaked on the oscilloscope trace.

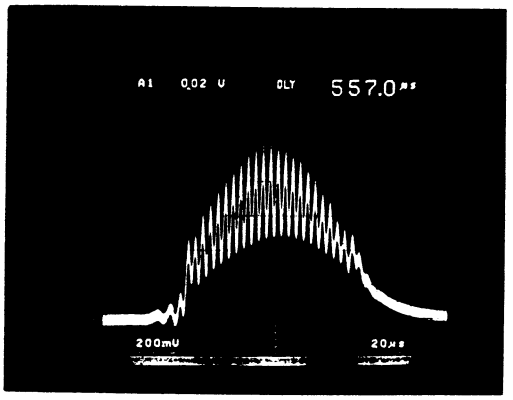

Fig. 3. Typical detector output signal with scanned fringe input.

The SPRITE detector packages used for these measurements consisted of a set of 700 μm bars with bifurcated readouts, a set of 400 μm bars with tapered readouts, and a set of multiple length bars with lengths of 450 - 650 μm and tapered readouts. Photographs of the 700 μm detectors and various length detectors are shown in Figs. 4 and 5, respectively. The three detector sets were produced from different boules of HgCdTe material so some variation in device characteristics could be expected.

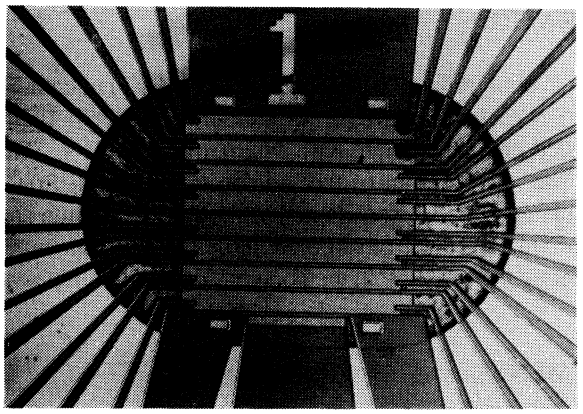

Fig. 4. Photograph of 700 μm SPRITE detectors with bifurcated readouts.

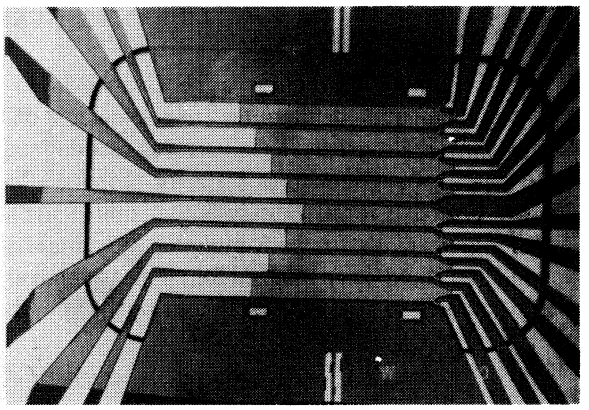

Fig. 5. Photograph of various length SPRITE detectors (450 μm - 650 μm) with tapered readouts.

Based on previous analyses of SPRITE detectors, the MTF depends on diffusion processes and detector readout geometry. For the along-scan direction, the diffusion MTF can be written as[4]

$$MTF_d(\xi,L) = \frac{1-\exp\left\{-[L_D^2(2\pi\xi)^2+1]\frac{L}{\mu E\tau}\right\}}{[L_D^2(2\pi\xi)^2+1]\left\{1-\exp\left[-\left(\frac{L}{\mu E\tau}\right)\right]\right\}}, \quad (2)$$

where ξ is the along-scan spatial frequency, L is the SPRITE bar length, L_D is the diffusion length, μ is the ambipolar mobility, τ is the carrier lifetime and E is the bias field. The MTF due to the readout alone is given by the Fourier transform of the y-profile of the readout as[5]

$$MTF_r(\xi) = \mathcal{F}\left[\text{rect}\left(\frac{x - X/2}{X} \right) \exp(-\alpha x) \right] . \quad (3)$$

The variables are: x is the along-scan length of the readout, X is the along-scan length of the readout, ξ is the along-scan spatial frequency, and α represents the taper coefficient of the readout. Total MTF can be expressed as a product of the diffusion and readout geometry MTFs as[6]

$$MTF = MTF_d \times MTF_r . \quad (4)$$

Measured and theoretical MTF curves for the 700 μm (bifurcated readout) and 400 μm (tapered readout) SPRITE bars are shown in Fig. 6, and Fig. 7 shows the measured and theoretical MTF of the 450 μm and 550 μm SPRITE bars (both with tapered readouts). The theoretical MTF curves were calculated from Eq. 4 using the values of the variables from Refs. 2 and 5 given in Table 1. The MTFs of the SPRITEs were normalized to unity at zero spatial frequency by dividing the measured output modulation depth by the input modulation depth of the fringes. The input modulation depth was measured with a 25 μm × 25 μm HgCdTe detector that was scanned across a stationary fringe of 1.0 cyc/mm. The measured modulation depth was then corrected by the value of the MTF of a 25 μm square detector at 1.0 cyc/mm, giving an input modulation depth of 0.94.

A comparison of measured MTFs versus theoretical MTFs in Figs. 6 and 7 indicate that although the analytical model is optimistic, there is good agreement regarding the dependence on bar length and readout geometry. Comparing MTF curves for two different pairs of structures (700 μm bifurcated and 400 μm tapered; and 450 μm and 550 μm tapered), we find that the difference in MTF as a function of spatial frequency is consistent between theoretical and experimental curves.

Table 1. Table of values used in calculation of theoretical MTF.

Carrier Lifetime	τ	15μsec
Hole Mobility	μ_h	150 $cm^2/V \cdot sec$
Hole Diffusion Constant	D_h	2.5 cm^2/sec
Hole Diffusion Length	L_D	61.2 μm
Electric Field	E	44.7 V/cm
Readout Length	X	62.5 μm
Taper Coefficient		
(tapered readout)	α	0.0228 μm^{-1}
(bifurcated readout)	α	0 μm^{-1}

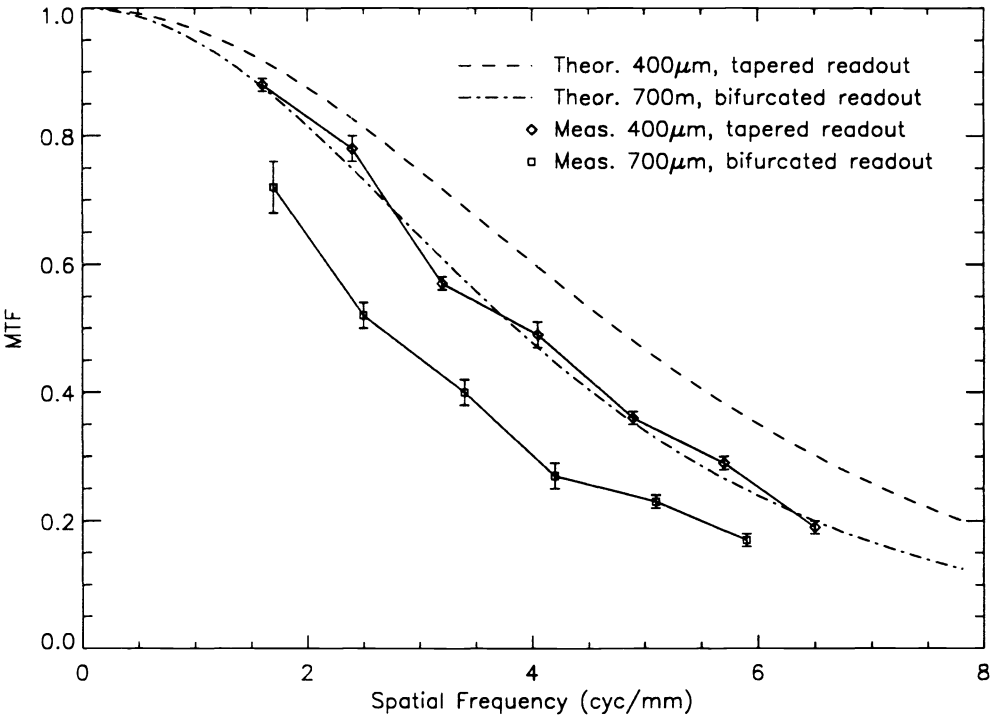

Fig. 6. Measured and theoretical MTF of 400 μm (tapered readout) and 700 μm (bifurcated readout) SPRITE detectors.

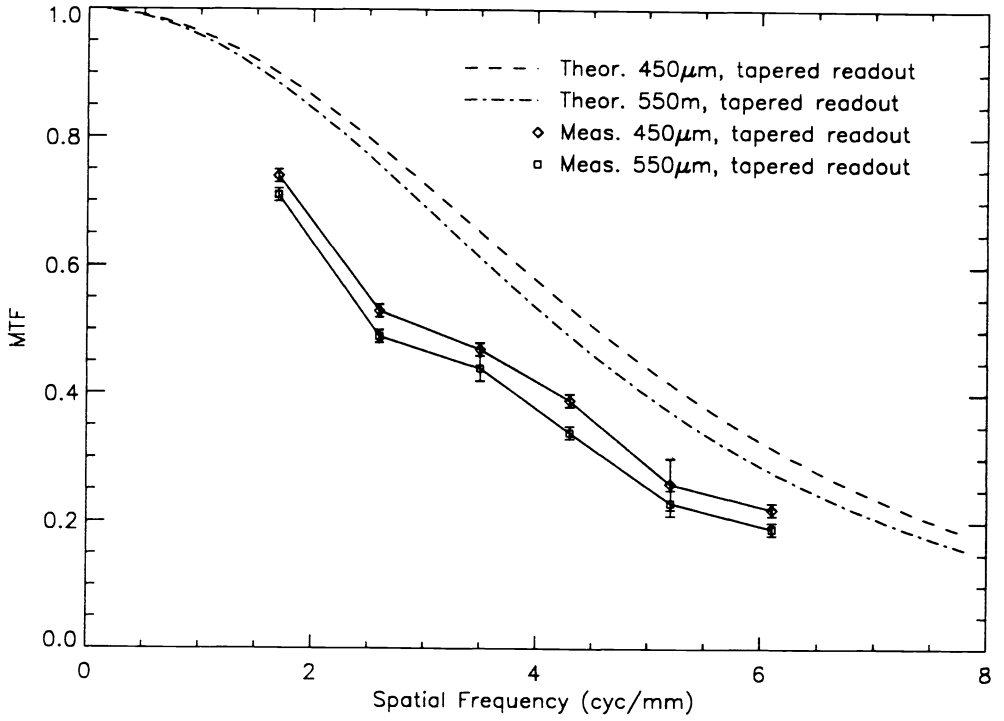

Fig. 7. Measured and theoretical MTF of 450 μm and 550 μm SPRITE detectors with tapered readouts.

5. CONCLUSIONS

The present theoretical model is obviously optimistic in the prediction of MTF performance. The only parameters which have so far been included in the model are those of carrier diffusion, bar length and readout geometry. Other effects will need to be included in the model to obtain more accurate predictions, such as carrier accumulation effects at the contacts[7] and the variation in ambipolar mobility resulting from the integration of background flux along the length of the SPRITE bar.[8]

Comparing the sine wave response method with other methods for measuring MTF of SPRITEs, such as the impulse response method[9,10] we find advantages and disadvantages to each method. The main disadvantage to the sine wave method is that different spatial frequencies require a separate measurement. Use of an impulse response measures MTF at all frequencies at once. One advantage of the sine wave method arises from the fact that the impulse response can drive the detector in a nonlinear fashion. The sine wave target projected onto the SPRITE is a closer approximation to an actual scene irradiance distribution. In addition, the sine wave method is capable of supplying a signal even at spatial frequencies which would be absent (or present only in small amout) from a focused spot input. This can be useful in increasing the SNR of these high frequencies in the measurement.

6. ACKNOWLEDGMENTS

This work was supported by McDonnell Douglas Missile Systems Company, Titusville Division and the Office of Naval Research/SDIO-IST under contract N0014-89-K-0125. Approved for public release; distribution is unlimited - Case No. 90-4172/L.

7. REFERENCES

1. C.T. Elliott, "New Detector for Thermal Imaging Systems," Electron. Lett. **17**, 312-313 (1981).
2. C.T. Elliot, D. Day, and D.J. Wilson, "An Integrating Detector for Serial Scan Thermal Imaging," Infrared Phys. **22**, 31-42 (1982).
3. D. Day and T.J. Shepherd, "Transport in Photo-conductors - I," Solid-State Electron. **25**, 707-712 (1982).
4. G. Boreman and A. Plogstedt, "Modulation transfer function and number of equivalent elements for SPRITE detectors," Appl. Opt. **27**, 4331-4335 (1988).
5. G. Boreman and A. Plogstedt, "Spatial filtering by a line-scanned nonrectangular detector: application to SPRITE readout MTF," Appl. Opt. **28**, 1165-1168 (1989).
6. T. Shepherd and D. Day, "Transport in Photo-conductors - II," Solid-State Electron. **25**, 713-718 (1982).
7. T. Ashley and C. Elliot, "Accumulation Effects at Contacts to n-type Cadmium-Mercury-Telluride Photoconductors," Infrared Phys. **22**, 367-376 (1982).
8. T. Ashley, C. Elliot, A. White, J. Wotherspoon, and M. Johns, "Optimization of Spatial Resolution in SPRITE Detectors," Infrared Phys. **24**, 25-33 (1984).
9. S.P. Braim and A.P. Campbell, "TED (SPRITE) Detector MTF," IEE Conference Publication **228**, 63-66 (1983).
10. B.K. Anderson, A.E. Plogstedt, and G.D. Boreman, "Impulse response measurements of SPRITE detector MTF," Proc. SPIE **1488** (1991).